

See discussions, stats, and author profiles for this publication at: <https://www.researchgate.net/publication/229222589>

Effects of fluorine-substitution on the molecular properties of dimethyl ethers: A theoretical investigation

ARTICLE *in* JOURNAL OF MOLECULAR STRUCTURE THEOCHEM · NOVEMBER 2007

Impact Factor: 1.37 · DOI: 10.1016/j.theochem.2007.06.023

CITATIONS

12

READS

23

3 AUTHORS:



Cam Pham

University of California, Davis

79 PUBLICATIONS 938 CITATIONS

SEE PROFILE



Minh Tho Nguyen

University of Leuven

748 PUBLICATIONS 10,861 CITATIONS

SEE PROFILE



Thérèse Zeegers-Huyskens

University of Leuven

208 PUBLICATIONS 2,984 CITATIONS

SEE PROFILE

Effects of fluorine-substitution on the molecular properties of dimethyl ethers: A theoretical investigation

Pham Cam Nam ^{a,b}, Minh-Tho Nguyen ^b, Thérèse Zeegers-Huyskens ^{b,*}

^a Faculty of Chemical Engineering, Danang University of Technology, 54 Nguyen Luong Bang, Danang City, Viet Nam

^b Department of Chemistry, 200F Celestijnenlaan, B-3001 Heverlee, Belgium

Received 10 May 2007; received in revised form 22 June 2007; accepted 23 June 2007

Available online 29 June 2007

Abstract

Quantum chemical calculations using density functional theory with the hybrid B3LYP functional and the 6-311++G(d,p) basis set were performed to determine the conformation of fluorinated ethers ($\text{CF}_n(\text{H}_{3-n})_2\text{O}$) with $n_F = 1$ to $n_F = 6$ and to evaluate the proton affinities of the O atoms and the deprotonation enthalpies of the CH bonds. Symmetric as well as asymmetric substituted ethers are investigated. The calculated results include the optimized geometries, natural bond orbital (NBO) data along with relevant vibrational frequencies. In all the fluorinated derivatives, except for CHF_2OCF_3 , the most stable conformation corresponds to a *gauche* orientation of the C–F bond relative to the C–H bond. The NBO analysis (occupation of σ^* antibonding orbitals, atomic charges and hyperconjugative energies) shows that the conformation is mainly governed by the anomeric (hyperconjugative) effect taking place through an electron transfer from the lone pair of the O atom to the $\sigma^*(\text{C}–\text{F})$ orbital. Electrostatic interaction between the non-bonded atoms may also stabilize the conformation. Protonation of the O site where the lone pair is tied up in the OH^+ bond results in marked changes of the geometry and occupation of antibonding orbitals. Large blue shifts of the CH stretching frequencies are also predicted in the protonated species. The results are in good agreement with the cancellation of the anomeric effect in the protonated species. Proton affinities of the most stable conformers range between 790 (CH_3OCH_3) and 580 (CF_3OCF_3) kJ mol^{-1} . Deprotonation enthalpies (DPE) of the CH bonds comprise between 1717 (CH_3OCH_3) and 1504 (CHF_2OCF_3) kJ mol^{-1} . The influence of fluoro-substitution on both C atoms is discussed. A rough correlation has been found between the DPE values and the % s-character of the C at the H atom involved in the deprotonation process.

© 2007 Elsevier B.V. All rights reserved.

Keywords: Fluorinated dimethyl ethers; B3LYP/6-311++G(d,p) calculations; Conformation; Protonation and deprotonation enthalpies

1. Introduction

It is well known that general anesthetics act by perturbing intermolecular interactions such as van der Waals complexes or hydrogen bonds without breaking or forming covalent bonds [1–5]. Their action depends on specific binding with proteins and therefore the knowledge of conformational, structural properties and hydrogen bond formation capacity of these compounds is very important. Anesthetics can form hydrogen bonds either as proton

donors or proton acceptors. It is now well recognised that CH groups are able to participate in a hydrogen bond and the strength of the resulting hydrogen bond is related to the hybridization (acidity) of the proton donor [6]. More specifically, molecules as chloroform (CHCl_3) or halothane ($\text{CF}_3\text{–CHClBr}$) are acting as weak CH proton donors and this has been shown by theoretical calculations or vibrational spectroscopy [7–9]. Examples of anesthetics acting as proton acceptors are ethers, the oxygen atom of which can act as a proton acceptor. Further, some anesthetics including halogenated ethers can function as proton donor and proton acceptor. In these molecules, one or several CH groups that can act as proton donors and the presence of several F (or Cl) atoms tend to make the CH bond

* Corresponding author. Tel.: +32 01622 86 23.

E-mail address: therese.zeegers@chem.kuleuven.be (T. Zeegers-Huyskens).

more acidic. This is the case for halogenated ethers such as enflurane ($\text{CHFCI}-\text{CF}_2-\text{O}-\text{CHF}_2$) [10–12]. Because the hydrogen bond properties are intimately related to both the proton acceptor ability of the O atom and the proton donor ability of the CH group, their knowledge is of fundamental importance.

The present work is a theoretical investigation of some of the fundamental properties of fluorinated derivatives of dimethyl ether. It should be mentioned that hydrofluoroethers are also being investigated because they are now considered as alternatives to chlorofluorocarbons, which have a potentially dangerous impact on the environment [13,14]. Since fluorinated ethers contain at least one carbon atom, OH radicals in the troposphere could oxidize them, or abstract H atoms. In this perspective, the CH bond dissociation enthalpies of the most stable conformers have been determined for several haloether molecules [15].

To the best of our knowledge, there are neither experimental nor theoretical data on the PAs of the oxygen atoms and the DPE of the CH bonds in fluorinated dimethylethers. These parameters have been calculated only for unsubstituted dimethylether [16,17].

The present paper is arranged as follows. Fluorinated ethers are characterized by different conformations and this will be discussed in the first part. The second part deals with their proton affinities. In the third part, the proton donor ability of the CH bonds will be discussed. The results reported here include the optimized geometries, relevant vibrational frequencies and results of a natural bond orbital (NBO) analysis of the isolated neutral molecules as well as of their protonated and deprotonated species.

2. Methods of calculation

The geometries of all the molecules studied and their corresponding protonated and deprotonated forms were fully optimized using density functional theory with the hybrid B3LYP functional, in conjunction with the 6-311++G(d,p) basis set. Frequency calculations were carried out at the same level to characterize the stationary points and also to estimate the zero-point energy (ZPE) and thermal corrections to the enthalpy. The proton affinities (PA) at the O sites were calculated at 298 K from the reaction enthalpies of the reactions $\text{B} + \text{H}^+ \rightarrow \text{BH}^+$. On a similar way, the deprotonation enthalpies of the CH bonds were calculated from the reaction enthalpies of the reactions $\text{B} \rightarrow \text{B}^- + \text{H}^+$. The enthalpy of each species was estimated from the electronic energy after taking into account the ZPE and other necessary corrections due to the rotational, translational and vibrational motions of the molecules. It must be mentioned that from the standpoint of efficiency and computational time, density functional methods are probably the most suitable approach for the calculations of PAs especially for large systems [18–21]. Charge on individual atoms, hybridization and hyperconjugative energies were obtained by using the natural bond orbital (NBO) population scheme [22]. The Gaussian 03 package

[23] was used for all the calculations analysed in the present work.

3. Results and discussion

3.1. Conformation of fluorinated dimethyl ethers (FDME)

The present study was intended to discuss the proton donor and proton acceptor abilities of the FDME. The optimization of the geometries revealed the existence of several stable conformers, all characterized by real frequencies. It seemed to us interesting to discuss in some details the characteristics of these conformers.

It is well known that the anomeric effects exert a strong influence on the conformational properties of organic molecules containing the segment $\text{R}-\text{X}-\text{C}-\text{Y}$, where X denotes an element which possesses one or more lone pairs which are antiperiplanar to the acceptor $\sigma^*(\text{C}-\text{Y})$ orbital, Y being an electronegative atom or group [24–28]. The origin of this effect is a negative hyperconjugation between the lone pair orbital(s) of X and the antibonding σ^* orbital of the C–Y bond. This corresponds to a *gauche* orientation of the C–Y bond relative to the X–R bond. As a consequence of this effect, the *gauche* conformation is predicted to be stabilized relative to the *trans* structure shown in Fig. 1. As it will be discussed in the present section, other effects such as the repulsion of the lone pair(s) and attraction or repulsion between non-bonded atoms can also influence the relative stability of the conformers.

It must be pointed out that the anomeric effect exists in dimethyl ether; more specifically, the role of lone-pairs interaction barriers has been thoroughly discussed [29–33]. At any level of calculations, the $\text{C}-\text{H}_g$ distances are longer than the $\text{C}-\text{H}_t$ ones. Calculations carried out at the BLYP/6-311G(d,p) level [34] gave C–H distances very similar to the ones reported in the present work.

The occupation of the $\sigma^*(\text{C}-\text{H})$ orbitals has a marked influence on the vibrational frequencies and infrared intensities of the $\nu(\text{C}-\text{H})$ stretching vibrations. It is often difficult to extract information about the nature of the different C–H bonds from the experimental spectra. Indeed, bands associated to normal modes are often described as mixed CH stretching vibrations. Moreover, extra bands can appear in the stretching region due to the occurrence of overtones showing intensity enhancement due to Fermi resonance [34]. An indirect way to examine the lone pair effect is to introduce a reagent that will inter-

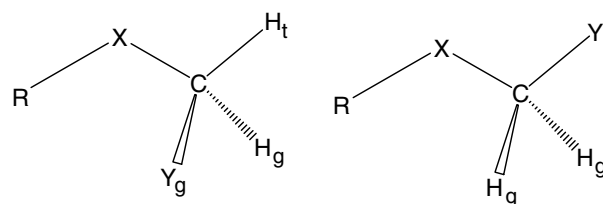


Fig. 1. *Gauche* (a) and *trans* (b) conformers of $\text{R}-\text{X}-\text{CH}_2\text{Y}$.

act with the O atom. In the hydrogen bond complexes between dimethyl ether and water or fluoroform, one of the O lone pairs of the ether molecule is involved in the $\text{OH}\cdots\text{O}$ or $\text{CH}\cdots\text{O}$ hydrogen bond. This interaction results in small experimental blue shifts between 8 and 12 cm^{-1} of the $\nu(\text{CH}_3)$ stretching vibration [35,36]. These experimental results are in good agreement with B3LYP/6-31G(d,p) calculations on the complex between dimethyl ether and water [37]. The shifted bands, usually referred as “Bohlmann bands” [38] give some experimental support for the existence of the lone pair effect. These bands are usually characterized by an increase of the infrared intensity with respect to the unperturbed vibrations. A proton will represent a stronger perturbation and our calculations show that protonation of dimethyl ether results in a much larger increase of the frequencies of the stretching vibrations. This point will be discussed in the next section.

Owing to the lower electronegativity of the H atom as compared with that of the F atom, the anomeric effect is expected to be weaker in dimethyl ether than in its fluorinated counterparts.

In FDME, the anomeric effect results in a shortening of the C–O bond and a lengthening of the C–F bond. Theoretical or experimental data are available only for $\text{CH}_3\text{OCH}_2\text{F}$ and CH_3OCF_3 . Results from microwave spectroscopy and ab initio calculations have shown that the *gauche* conformation of $\text{CH}_3\text{OCH}_2\text{F}$ is preferred over the *trans* counterpart [39–41]. There exists only one possible conformer for CH_3OCF_3 ; gas phase diffraction measurements, microwave spectroscopy and theoretical calculations have shown that the hyperconjugation results in this case in two different bond lengths, namely, the C–F_g bond being by 0.018 \AA longer than the C–F_t one [42]. The optimized geometrical parameters, relevant bond angles and total energies of the stable conformers of FDME are shown in Fig. 2. This Figure also indicates the C–O distances and COC bond angles in dimethyl ether useful for a further comparison with its fluorinated counterparts. The C1–O, C2–O, C1–F and C2–F distances in these stable conformers and the relative energies are reported in Table 1. It must also be noticed that when the H atoms are in *trans* conformation, the CH distances vary between 1.075 and 1.0890 \AA . The CH distances are slightly longer when the H atoms are in *gauche* conformation, varying from 1.0910 to 1.0996 \AA . The hybridization of the C atoms bonded to hydrogen atoms will be discussed in more details in the next sections.

Inspection of the results of Table 1 reveals that when the number of F atoms comprises between one and three, the most stable conformer is characterized by two H atoms in *trans* position. In this conformation, there is no repulsion between the lone pairs(s) of the F and O atoms. When the number of F atoms is equal to four, in the symmetrical as well in the asymmetrical derivatives, only one H atom occupies the *trans* position. In contrast, when the number of F atoms is equal to five, two F atoms are in a *trans* position, the H atom being in a *gauche* position.

The difference in relative stability of both the A and B conformers of $\text{CH}_3\text{OCH}_2\text{F}$ being the largest (19 kJ mol^{-1}) among the studied derivatives, we will discuss more in details the properties of these two derivatives. Table 2 contains parameters allowing us to discuss the differences between the A and B conformers, namely the C–H distances and some relevant NBO parameters such as the NBO charges, the occupation of σ^* orbitals along with hyperconjugative energies from the O or F atoms to antibonding orbitals.

The optimized C–H distances are slightly different in the two conformers. We note that there is no marked difference between the hybridization of the C atom bonded to the hydrogen atoms. The % s-character of the C1 atom ranges indeed between 25.8 and 26.6 and the % s-character of the C2 atom varies between 27.4 and 27.6 in both conformers. The largest difference in the hybridization in the two conformers is predicted for the oxygen lone pair taking a value of 41.7% s-character in the A conformer and of 45.5% in the B conformer.

Comparison of the NBO data for both conformers A and B provides a nice illustration of the hyperconjugative effect. At first, the delocalization of the charges taking place from O to F results in a smaller negative charge on the O atom (by $0.014e$) and a larger negative charge on the F atom (by $0.031e$) in the A conformer than in the B one. The polarity of the C2–O bond is also larger in B than in A. Let us also notice that in both conformers, the positive charge on the H_t atom of the CH_3 group is larger, by $0.017e$ (in A) and $0.033e$ (in B) than the charge on the H_g atom. The largest difference in the occupation of the σ^* antibonding orbital is predicted for the C–F bond, which decreases from 0.077 to $0.035e$ on going from A to B. Further, in B, the occupation of the $\sigma^*(\text{C–H})$ orbitals is larger than in A, the largest difference being predicted for the C2–H_t bond, the σ^* occupation increasing from 0.0264 to $0.0405e$ on going from A to B. As expected, the hyperconjugative energy for the transfer $\text{LP}(1)\text{ O} \rightarrow \sigma^*(\text{C–F})$ is markedly larger for A (81.2 kJ mol^{-1}) than for B (22.6 kJ mol^{-1}). The large occupation of the $\sigma^*(\text{C–F})$ orbital and the large hyperconjugative energy $\text{LP O}(1) \rightarrow \sigma^*(\text{C–F})$ are both in agreement pointing toward an anomeric effect favoring the most stable A conformer.

Interestingly, there is an hyperconjugative energy of 29.7 kJ mol^{-1} from the second O lone pair to the $\sigma^*(\text{C2–H}_g)$ orbital in the B conformer. This shows that a hyperconjugation of the second O lone pair to the C–H bond in the *gauche* position also stabilizes the B conformer, but to a lesser extent than the $\text{LP}(1)\text{ O} \rightarrow \sigma^*(\text{C–F})$ hyperconjugation in the A conformer. This effect is in line with the greater occupation of the $\sigma^*(\text{C2–H}_g)$ orbital in B than in A. This results in a longer the C2–H_g distance in the B conformer (1.0996 \AA) than in the A conformer (1.0979 \AA).

We must also notice that in both conformers, there is also a small hyperconjugative energy from the O lone pair(s) to the C2 Rydberg orbitals, ranging from 4 to 17 kJ mol^{-1} . A hyperconjugation from the $\text{LP}(2)\text{ F}$ atom

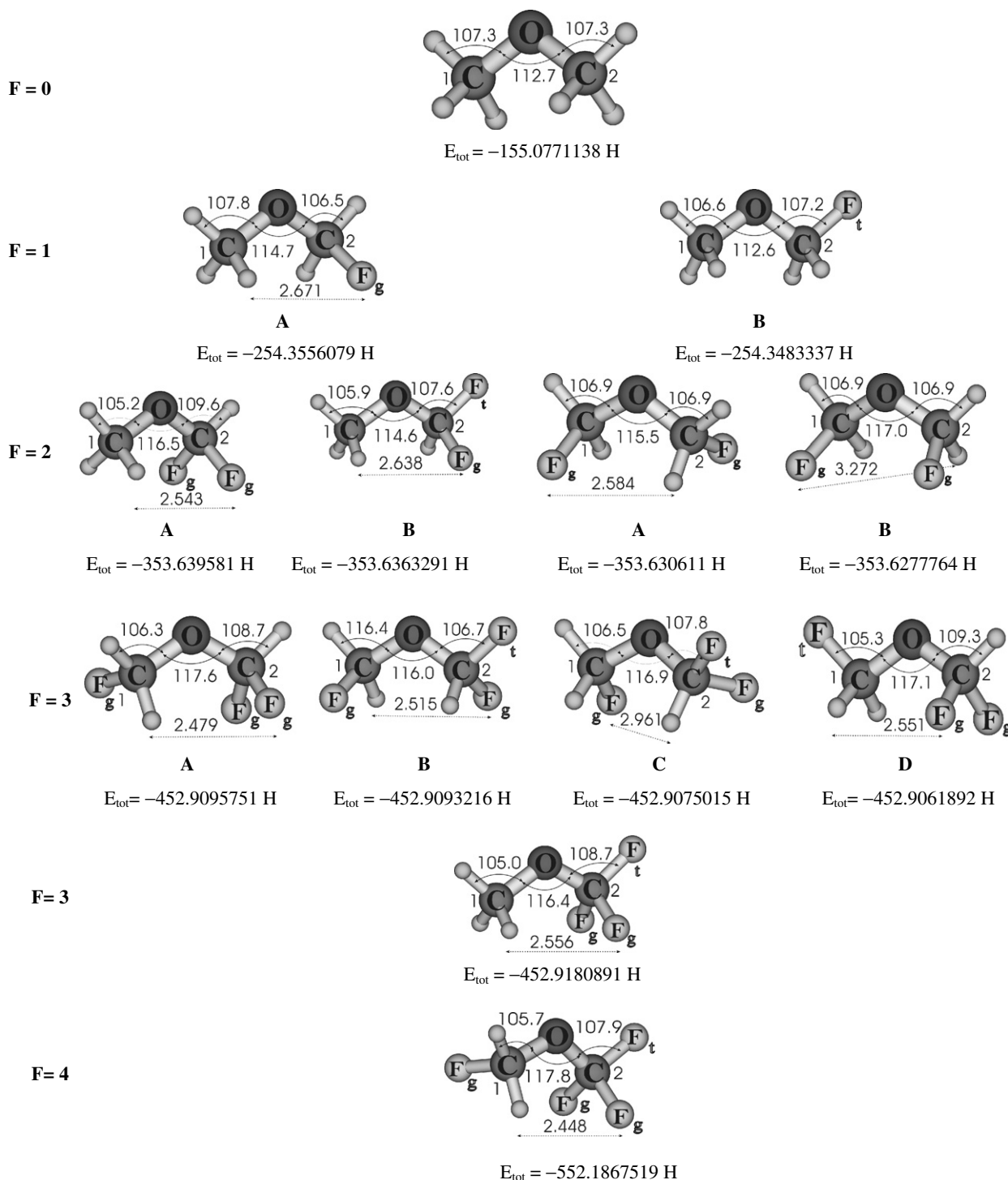


Fig. 2. B3LYP/6-311++G(d,p) optimized geometrical parameters and total energies (in hartree) of the stable conformers of fluorinated dimethyl ethers.

to the C2 Rydberg orbital of 28 kJ mol^{-1} is also predicted for B.

The lone pair effect results in different vibrational frequencies for the A and B conformers of $\text{CH}_3\text{OCH}_2\text{F}$. Indeed, the wavenumbers of the $\nu(\text{C1H}_3)$ vibrations are predicted at 3136, 3075 and 2999 cm^{-1} in the A conformer and at 3134, 3029 and 2984 cm^{-1} in the B conformer. We must note that in both conformers, three

stretching modes are predicted, indicating a breaking of the C_{3v} local symmetry due to the non-equivalent C–H bonds. The two components of the $\nu^{\text{as}}(\text{C1H}_3)$ vibrations and the $\nu^{\text{s}}(\text{C1H}_3)$ vibrations are shifted by 2, 46 and 15 cm^{-1} , respectively. The same remark also holds for the $\nu^{\text{as}}(\text{C2H}_2)$ and $\nu^{\text{s}}(\text{C2H}_2)$ vibrations which are computed at 3113 and 2990 cm^{-1} , respectively in A and at 3015 and 2967 cm^{-1} , respectively in B. The $\nu^{\text{s}}(\text{C2H}_2)$

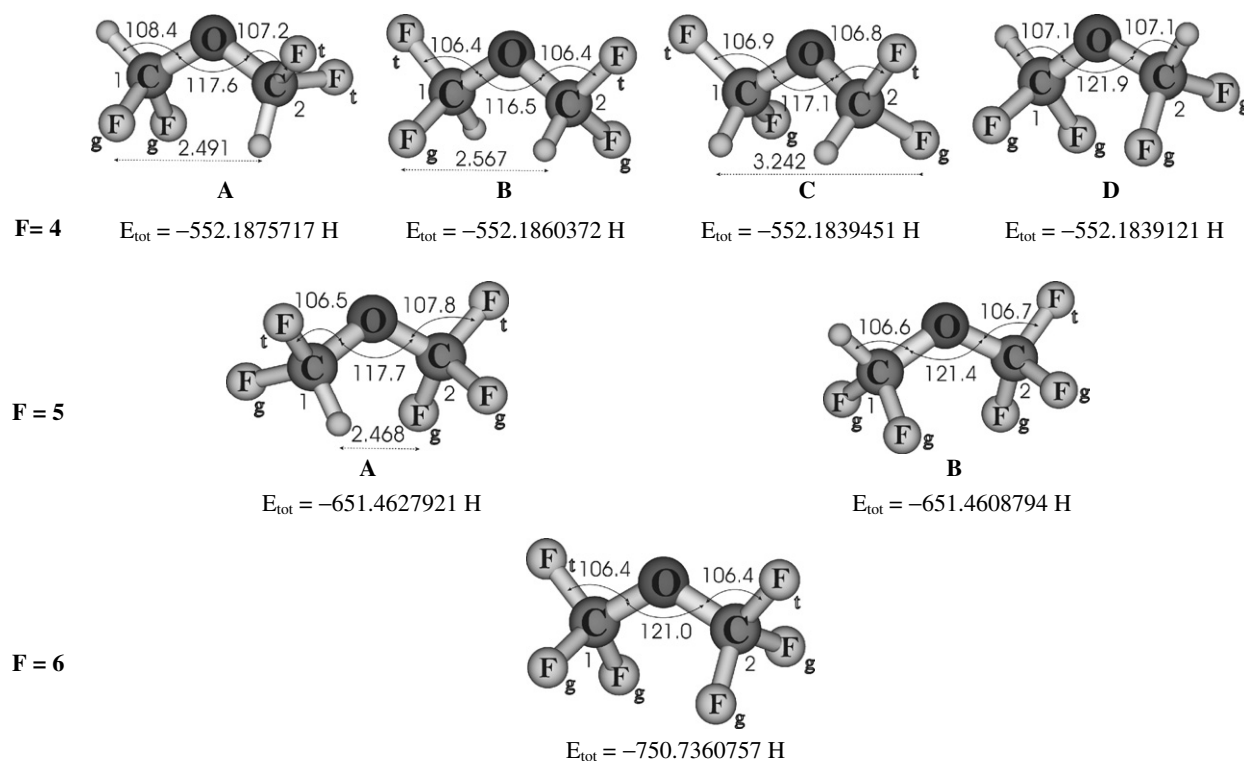


Fig. 2 (continued)

Table 1

Relative energies (ΔE in kJ mol^{-1}), C–C and C–F distances (\AA) in dimethyl ether and its fluorinated derivatives estimated at the B3LYP/6-311++G(d,p) level

Compound	ΔE	C1–O	C2–O	C1–F _g	C1–F _t	C2–F _g	C2–F _t
CH ₃ OCH ₃	0	1.413	1.413				
CH ₃ OCH ₂ F (A)	0	1.427 ^a	1.372 ^a			1.398 ^a	
CH ₃ OCH ₂ F (B)	19.0	1.420	1.389				1.373
CH ₃ OCHF ₂ (A)	0	1.445	1.345			1.376	
CH ₃ OCHF ₂ (B)	8.5	1.434	1.354			1.380	1.350
CH ₂ FOCH ₂ F (A)	0	1.390	1.390	1.395		1.395	
CH ₂ FOCH ₂ F (B)	7.5	1.389	1.389	1.386		1.386	
CH ₃ OCF ₃		1.444 ^b	1.336 ^b			1.357	1.333 ^b
CH ₂ FOCHF ₂ (A)	0	1.408	1.365	1.379		1.371	
CH ₂ FOCHF ₂ (B)	0.7	1.395	1.375	1.391		1.375	1.361
CH ₂ FOCHF ₂ (C)	5.4	1.392	1.373	1.385		1.373	1.357
CH ₂ FOCHF ₂ (D)	8.9	1.364	1.351	1.364		1.373	
CH ₂ FOCF ₃ ^c		1.411	1.356	1.375		1.353	1.330
CHF ₂ OCHF ₂ (A)	0	1.392	1.369		1.348	1.362	
					1.352	1.365	
CHF ₂ OCHF ₂ (B)	4.2	1.384	1.384	1.353		1.353	
CHF ₂ OCHF ₂ (C)	9.6	1.379	1.379	1.357	1.345	1.358	1.343
CHF ₂ OCHF ₂ (D)	9.7	1.382	1.382	1.368	1.339	1.367	1.340
CHF ₂ OCF ₃ (A)	0	1.398	1.361	1.350		1.349	1.325
CHF ₂ OCF ₃ (B)	5.0	1.390	1.374	1.352		1.339	1.331
CF ₃ OCF ₃		1.380	1.380	1.337	1.326	1.337	1.326

^a The C1–O, C2–O and C–F distances determined by microwave spectroscopy are 1.426, 1.368 and 1.395 Å, respectively [40].

^b The C1–O, C2–O, C–F_g and C–F_t distances calculated at the MP2/6-31G(d,p) level are 1.438, 1.345, 1.353 and 1.333 Å, respectively [41].

^c Only one stable conformation is predicted by our calculations.

vibration is by 98 cm^{-1} lower in B than in A. Although infrared intensities calculated at this level of theory only represent qualitative trends [43], the predicted infrared

intensity of this last mode, equal to 41 km mol^{-1} in A and to 85 km mol^{-1} in B, is in agreement with the expectations.

Table 2
Comparison between the A and B conformers of CH₃OCH₂F and protonated CH₃OCH₂F (A)

	CH ₃ OCH ₂ F (A)	CH ₃ OCH ₂ F (B)	CH ₃ OH ⁺ CH ₂ F (A)
<i>CH distances^c (Å)</i>			
C1–H _t	1.0887	1.0885	1.0868
C1–H _g	1.0930, 1.0979	1.0982	1.0884
C2–H _t	1.0903		1.0890
C2–H _g	1.0987	1.0996	1.0882
<i>NBO charge (e)</i>			
O	−0.573	−0.587	−0.525
C1	−0.209	−0.209	−0.188
C2	0.385	0.410	0.403
F	−0.407	−0.376	−0.313
H (C1)	0.161 ^a , 0.178 ^a , 0.188 ^b	0.161 ^a , 0.194 ^b	0.225 ^a , 0.232 ^b
H (C2)	0.123 ^a , 0.153 ^b	0.123 ^c	0.195, 0.199
H ⁺			0.547
<i>Occupation σ* orbital (e)</i>			
C1–O	0.0116	0.0082	0.0144
C2–O	0.0344	0.0361	0.076
C–F	0.0769	0.0349	0.0239
C1–H _t	0.0088	0.0095	0.0030
C1–H _g	0.0165, 0.0177	0.0213	0.0043, 0.0063
C2–H _t	0.0264		0.0219
C2–H _g	0.0344	0.0405 ^d	0.0234
O–H ⁺			0.011
<i>Hyperconjugative energies (kJ mol^{−1})</i>			
LP (1) O → σ*(C–F)	81.1	22.6	
LP (1) O → σ*(C2–H _g)	9.5	29.7	
LP (2) O → σ*(C1–H _g)	17.6, 25.9	25.9	4.4, 9.1
LP (3) F → σ*(C2–O)	40.9	43.9	80.1

C–H distances and relevant NBO data.

^a H atom in *gauche* position.

^b H atom in *trans* position.

^c The two C2–H_g bonds are equivalent.

^d The two C2–H_g bonds are equivalent.

^e The CH distances are indicated by four digits. This is justified by the fact that in a future work, we will investigate the hydrogen bond complexes involving DMFE and guest molecules. The variations of the CH distances in the weak complexes involving CH bond are very often of the magnitude of 0.1–0.5 mÅ.

It is also worth mentioning that the vibrational mode predicted at 988 cm^{−1} with an infrared intensity of 200 km mol^{−1} has a predominant ν(C–F) character. This vibrational mode is calculated at 1090 cm^{−1} with an infrared intensity of 170 km mol^{−1}. These spectroscopic characteristics are related to the shorter C–F bond and the smaller σ*(C–F) occupation in B.

The NBO analysis carried out for the two CH₃OCH₂F conformers can throw some light on the other fluorinated ethers. As a general rule, the differences between the C1–O and C2–O distances in asymmetrically substituted molecules decrease with increasing relative energies (see the results of Table 1). This is the case for the four conformers of CH₂FOCHF₂, where the differences between the two C–O distances equal to 0.043, 0.020, 0.019 and 0.013 Å, respectively, are ordered according the relative energies equal to 0, 0.7, 5.4 and 8.9 kJ mol^{−1}. For all the derivatives, the C–F_g distances are by 0.015–0.030 Å longer than the C–F_t distances.

Finally, the molecules may be stabilized by an electrostatic attraction between the H and F atoms that are both

in *gauche* position. As indicated in Fig. 1, the intramolecular H_g...F_g distances are in several conformers, relatively short (between 2.5 and 2.6 Å). This distance is even shorter in the CHF₂OCF₃ (A) conformer (2.468 Å). The electrostatic attraction between the positively charged H_g atom (0.141e) and the negatively charged F atom (−0.346e) can provide an explanation for the greater stability of this conformer compared with the B one where the two C1–F bonds are in *gauche* position. It should be noted that in this molecule, the hyperconjugation from the second O lone pair to the σ*(C1–H_g) orbital may also contribute to the stabilization of the *trans* conformer.

3.2. Protonated fluorinated dimethyl ethers

This section is dealing with the protonated A conformers of the investigated DMFE. In the protonated forms, the O lone pair atom is tied up in the oxygen–proton bond. The optimized geometries (C1OC2 and C1OHC2 bond angles) of the protonated molecules are shown in Fig. 3. The optimized C–O and C–F distances are

reported in Table 3. As shown in earlier works [44–46], protonation of cyclic and acyclic ethers results in a marked elongation of the C–O bond. MP2/6-31G(d) calculations predicted a variation of the C–O distance from 1.391 to 1.479 Å on going from isolated CH_3OCH_3 to its protonated species. There is also a marked increase of the C–O–C angle of ca. 6° [11,29]. Our B3LYP calculations predicting for this molecule an elongation of 0.084 Å and a COC angle increase of 5.5° are in good agreement with these earlier data.

The results of Table 3 indicate that for all the fluorinated ethers studied in the present work, protonation results in a marked elongation of both C–O bonds along with an opening of the C1OC2 angle. The COH^+ angles vary within small limits, between 112° and 113° but the COH^+C dihedral angles increase with the number of F atoms, varying from 135° (number of F = 1) to 146° (number of F = 6).

In order to have a better insight into the protonation process, we consider a set of more extensive data for the protonated $\text{CH}_3\text{OCH}_2\text{F}$, whose conformation has been discussed in details in the previous section. The CH distances and the NBO parameters in $\text{CH}_3\text{OH}^+\text{CH}_2\text{F}$ (A) are summarized in Table 2. As expected, protonation of the O atom results in a decrease of the negative charge on the O and F atoms, the decrease on the latter atom being about 0.1e. All the H atoms bonded to the C1 and C2 atoms experience an increase of the positive charge. This increase indicates that the charge transfer from the $\text{CH}_3\text{OCH}_2\text{F}$ to the proton equal to 0.45e takes place at the expense of all the atoms in the molecule. Protonation also induces a marked decrease of the $\sigma^*(\text{C}-\text{F})$ occupation by more than 0.06e. Interestingly, the $\text{C2}-\text{H}_g$ bond becomes slightly shorter (1.0882 Å) than the $\text{C2}-\text{H}_t$ one (1.0890 Å). This is the only case, at least for the compounds studied in the present work, where the $\text{C2}-\text{H}_g$ bond becomes shorter than the $\text{C2}-\text{H}_t$ one.

For the remaining derivatives studied in the present work, we will now consider the fluorinated ethers bearing a CH_3 group, namely $\text{CH}_3\text{OCH}_2\text{F}$, CH_3OCHF_2 and CH_3OCF_3 . Protonation results in an increase of the C1–O distance, ranging from 0.078 to 0.085 Å, very similar to the effect predicted for CH_3OCH_3 . Protonation effects of the C2–O distances are larger and roughly depend on the number of F atoms implanted on the C2 atom, taking values of 0.121 Å for $\text{CH}_3\text{OCH}_2\text{F}$, 0.169 Å for CH_3OCHF_2 and 0.172 Å for CH_3OCF_3 . Protonation effects on the contraction of the $\text{C2}-\text{F}_g$ distance are roughly constant and vary between 0.051 and 0.068 Å. The elongation of the C2–O bond and the contraction of the vicinal $\text{C2}-\text{F}$ bond both indicate both the cancellation of the hyperconjugation effect upon protonation. Similar effects are predicted for the other fluorinated ethers. In the $\text{CH}_2\text{F}-\text{O}$ series, the elongation of the C2–O bonded between 0.013 and 0.181 Å; the contraction of the $\text{C2}-\text{F}_g$ bond comprises between 0.054 and 0.064 Å and is of the same order of magnitude as

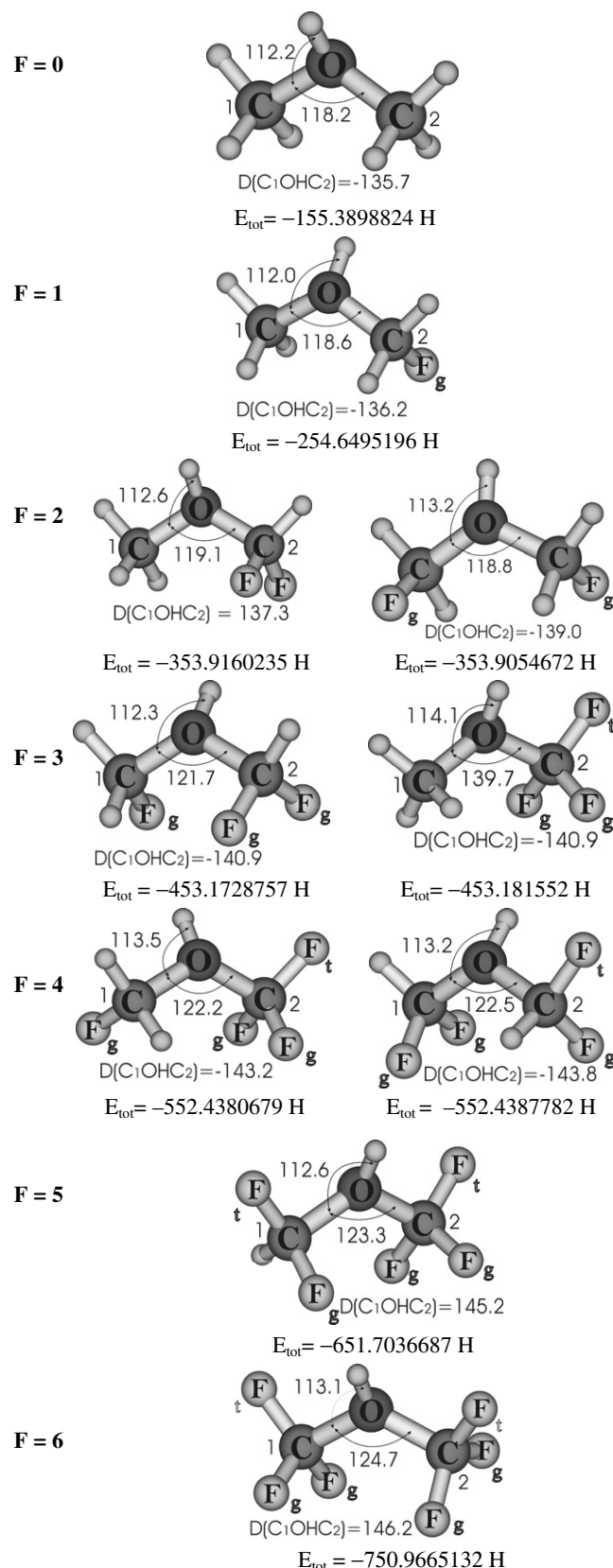


Fig. 3. B3LYP/6-311++G(d,p) optimized geometrical parameters of the protonated fluorinated dimethyl ethers (A conformers).

in the other fluorinated ethers. The OH^+ distances slightly increase with the number of F atoms and range

Table 3
C–O, C–F and OH⁺ distances (Å) in the most stable protonated conformers of fluorinated dimethyl ethers^{a,b}

Protonated molecule	C1–O	C2–O	C1–F _g	C2–F _g	OH ⁺
CH ₃ OCH ₃	1.497(+0.084)	1.497(+0.084)			0.9725
CH ₃ OCH ₂ F	1.512(+0.085)	1.493(+0.121)		1.337(−0.061)	0.9754
CH ₃ OCHF ₂	1.523(+0.078)	1.514(+0.069)		1.308(−0.068)	0.9761
				1.317(−0.059)	
CH ₂ FOCH ₂ F	1.505(+0.115)	1.534(+0.134)	1.323(−0.072)	1.335(−0.060)	0.9766
CH ₃ OCF ₃	1.525(0.081)	1.508(0.172)		1.301(−0.056)	0.9783
				1.306(−0.051)	
CH ₂ FOCHF ₂	1.529(+0.121)	1.546(+0.181)	1.326(−0.057)	1.307(−0.064)	0.9785
CH ₂ FOCF ₃	1.540(+0.129)	1.531(+0.175)	1.322(−0.043)	1.299(−0.054)	0.9803
CHF ₂ OCHF ₂	1.572(+0.180)	1.539(+0.170)	1.303 ^c (−0.064)	1.307(−0.041)	0.9811
CHF ₂ OCF ₃	1.605(+0.207)	1.519(+0.158)	1.297(−0.053)	1.302(−0.047)	0.9823
CF ₃ OCF ₃	1.563(+0.183)	1.572(+0.192)	1.286 ^d (−0.051)	1.291 ^d (−0.046)	0.9814
			1.296 ^e (−0.041)	1.294 ^e (−0.043)	

^a The numbers in parentheses indicate the variations with respect of the isolated molecule.

^b In some of the protonated molecules, two different C1–F or C2–F distances are predicted; only the distances that differ by more than 0.05 Å are indicated in this Table.

^c C–F bond in *gauche* position.

^d C–F bond in *gauche* position.

^e C–F bonds in *trans* position

between 0.9725 Å (number of F = 0) and 0.9814 Å (number of F = 6).

The proton affinities (PA) of the most stable conformers are indicated in Table 4.

The PA of CH₃OCH₃ calculated at the MP2/6-31G(d)//HF//HF/6-31G(d) level is nearly the same (792 kJ mol^{−1}) [16] as the present value which justifies our computational method and level. No experimental or theoretical data are available for the other derivatives. Our results show that on going from CH₃OCH₃ to its hexafluoro-derivative, the PA decreases by 210 kJ mol^{−1}. Approximately the same substituent effect is found in fluorinated acetone. Accordingly, the PA of unsubstituted acetone is equal to 823 kJ mol^{−1} and amounts to of 628 kJ mol^{−1} in hexafluoroacetone [17].

Inspection of the data of Table 4 reveals the PA values decrease with the number of F atoms implanted on the C atoms but are nearly independent on the site of substitution. The results indicate further that the effect of each electronegative substitution decreases with the number of F atoms present. The influence of a first F atom inducing a decrease of the PA of ca 48 kJ mol^{−1} is larger than the influence of the fifth F atom (decrease of the PA of ca 30 kJ mol^{−1}) showing certain saturation effect.

Table 5 contains the calculated frequencies of some relevant vibrational modes, namely the ν(OH⁺), ν(CH)

stretching vibrations along with the γ(OH⁺) (out-of-plane deformation). The frequencies of the ν(OH⁺) vibrations predicted between 3717 and 3615 cm^{−1} decrease with the number of F atoms implanted on the C atoms. As indicated in Fig. 4, the vibrational frequencies are linearly correlated to the r(OH⁺) distances:

$$\nu(\text{OH}^+) = 14.75 \times 10^3 - 11.35 \times 10^3 r(\text{OH}^+) \quad (r = 0.9896) \quad (1)$$

In some of the protonated molecules, the γ(OH⁺) vibrations are coupled with other vibrational modes. Nevertheless, their frequencies follow the same trend as the ν(OH⁺) vibrations.

As indicated in Table 5, protonation results in large perturbations of the CH stretching modes which are all blue-shifted with respect to the neutral molecules. Owing to the mixed character of these modes, the shifts can be evaluated by considering the average of the frequencies in the neutral and protonated molecules. For the CH₃OCH₂F molecule as for example, protonation induces blue shifts of ca 100 cm^{−1} for both the ν(C1H₃) and ν(C2H₂) vibrations. Protonation also results in a spectacular decrease of the infrared intensities taking in some of derivatives values as low as 1 km mol^{−1}. These spectroscopic effects are in agreement with the cancellation of the lone pair effect in the protonated species.

3.3. Deprotonation enthalpies of fluorinated dimethyl ethers

Deprotonation results in marked changes of the distances and angles. If deprotonation takes place at the C1 atom, the C1–O distance markedly increases and the C2–O distance decreases. The remaining C–H distances also increase. These changes will no more be discussed hereafter. The deprotonation enthalpies (DPE) of FDME are

Table 4
Proton affinities at 298 K of the A conformers of fluorinated dimethyl ethers (kJ mol^{−1}) calculated using the B3LYP/6-31++G(d,p)+ZPE level

Compound	PA	Compound	PA
CH ₃ OCH ₃ ^a	791.0	CH ₃ OCF ₃	665.2
CH ₃ OCH ₂ F	743.5	CHF ₂ OCHF ₂	645.0
CH ₂ FOCH ₂ F	703.8	CH ₂ FOCF ₃	634.6
CH ₃ OCHF ₂	707.7	CHF ₂ OCF ₃	643.6
CH ₂ FOCHF ₂	666.3	CF ₃ OCF ₃	580.2

^a The experimental PA value is 804 kJ mol^{−1} (Ref. [17]).

Table 5

Vibrational frequencies (cm^{-1}) in the A conformers of neutral and protonated fluorinated dimethyl ethers obtained from B3LYP/6-311++G(d,p) calculations

	$\nu(\text{OH}^+)$	$\nu(\text{CH})^a$	$\gamma(\text{OH}^+)$
CH_3OCH_3		3113(21), 3112(32), 3010(1), 3006(144), 2971(66), 2959(60)	
$\text{CH}_3\text{OH}^+\text{CH}_3$	3717	3206(3), 3194(2), 3079(2)	630
$\text{CH}_3\text{OCH}_2\text{F}$		3136(21), 3112(41), 3075(37), 2999(75), 2991(50)	
$\text{CH}_3\text{OH}^+\text{CH}_2\text{F}$	3681	3210(2), 3209(4), 3198(1), 3105(3), 3086(1)	623
$\text{CH}_2\text{FOCH}_2\text{F}$		3153(23), 3150(14), 3070(6), 3065(64)	
$\text{CH}_2\text{FOH}^+\text{CH}_2\text{F}$	3653	3198(1), 3194(1), 3103(5), 3101(2)	582, 493 ^b
CH_3OCHF_2		3159(11), 3148(28), 3127(16), 3051(29)	
$\text{CH}_3\text{OH}^+\text{CHF}_2$	3677	3224(5), 3213(5), 3154(2), 3091(1)	592
CH_3OCF_3		3167(7), 3130(14), 3052(24)	
$\text{CH}_3\text{OH}^+\text{CF}_3$	3649	3220(5), 3213(7), 3088(1)	516, 400 ^b
$\text{CH}_2\text{FOCHF}_2$		3158(21), 3155(17), 3083(26)	
$\text{CH}_2\text{FOH}^+\text{CHF}_2$	3647	3212(3), 3159(2), 3111(3)	503, 387 ^b
$\text{CHF}_2\text{OCHF}_2$		3168(18), 3136(14)	
$\text{CHF}_2\text{OH}^+\text{CHF}_2$	3616	3189(2), 3158(2)	517
CH_2FOCF_3		3163(11), 3084(23)	
$\text{CH}_2\text{FOH}^+\text{CF}_3$	3625	3209(3), 3108(3)	541
CHF_2OCF_3		3129(15)	
$\text{CHF}_2\text{OH}^+\text{CF}_3$	3602	3184(3)	484
$\text{CF}_3\text{OH}^+\text{CF}_3$	3615		374

^a The numbers in bold characters indicate the vibrations of the CH_3 group; the numbers in parentheses indicate the infrared intensities in km mol^{-1} .

^b Two vibrational modes with predominant $\gamma(\text{OH}^+)$ character.

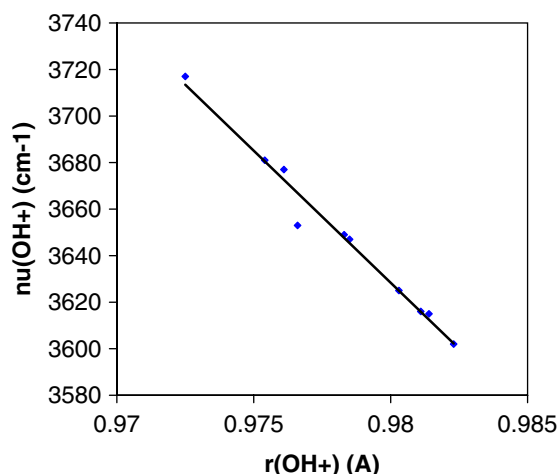


Fig. 4. The vibrational frequencies $\nu(\text{OH}^+)$ (cm^{-1}) as a function of the distances $r(\text{OH}^+)$ (Å), in protonated fluorinated dimethyl ethers.

reported in Table 6 which also contains the % s-character of the C atom bonded to the hydrogen atom involved in the protonation process along with the occupation of the corresponding $\sigma^*(\text{C-H})$ orbital in the neutral molecules. It can be argued that NBO data are very sensitive to the level of theory used in the calculations and that the comparison between different molecules is only meaningful as long as the same level of theory is used. However, we note that earlier B3LYP calculations for dimethyl ether carried out with the smaller 6-31G(d) basis set give % s-character and $\sigma^*(\text{C-H})$ occupation equal to 26.05 and 0.0245e [23], respectively, that are very similar to the values calculated in the present work. This gives some support for the present data.

Table 6

Deprotonation enthalpies (kJ mol^{-1}), % s-character of the $\text{C} \rightarrow \text{H}$ bonds and occupation of the $\sigma^*(\text{C-H})$ orbitals (e)

	DPE	%s ($\text{C} \rightarrow \text{H}$)	$\sigma^*(\text{C-H})$
$\text{CH}_3^i\text{OCH}_3$	1717.6 ^a	25.65	0.0099
$\text{CH}_3^g\text{OCH}_3$	1716.9	25.96	0.0229
$\text{CH}_3^i\text{OCH}_2\text{F}$	1674.4	25.85	0.0088
$\text{CH}_3^g\text{OCH}_2\text{F}$	1671.6, 1670.6	26.05, 26.55	0.0166, 0.0177
$\text{CH}_3^g\text{OCH}_2^g\text{F}$	1677.8	27.40	0.0264
$\text{CH}_3^g\text{OCH}_2^g\text{F}$	1670.8	27.64	0.0344
$\text{CH}_2^i\text{FOCH}_2\text{F}$	1635.4	27.63	0.0251
$\text{CH}_2^g\text{FOCH}_2\text{F}$	1630.3	28.23	0.0309
$\text{CH}_3^i\text{OCHF}_2$	1650.8	25.95	0.0081
$\text{CH}_3^g\text{OCHF}_2$	1640.7	26.73	0.0136
$\text{CH}_3\text{OCH}^i\text{F}_2$	1611.2	29.59	0.0435
$\text{CH}_3^i\text{OCF}_3$	1633.4	26.01	0.0080
$\text{CH}_3^g\text{OCF}_3$	1629.9	26.76	0.0133
$\text{CH}_2^i\text{FOCHF}_2$	1612.4	27.65	0.0263
$\text{CH}_2^g\text{FOCHF}_2$	1608.3	28.48	0.0277
$\text{CH}_2\text{FOCH}^i\text{F}_2$	1572.1	29.88	0.0432
$\text{CH}^i\text{F}_2\text{OCHF}_2^b$	1534.1	30.10	0.0426
$\text{CH}^g\text{F}_2\text{OCHF}_2$	1540.5	30.52	0.0450
$\text{CH}_2^i\text{FOCF}_3$	1589.0	27.75	0.0259
$\text{CH}_2^g\text{FOCF}_3$	1580.4	28.44	0.0281
$\text{CH}^g\text{F}_2\text{OCF}_3$	1503.9	30.53	0.0459

The bold characters indicate the deprotonation site.

^a The experimental value is $1703 \pm 8 \text{ kJ mol}^{-1}$.

^b This DPE corresponds to the D conformer in the neutral molecule (Fig. 2). The structure of the deprotonated A conformer could not be optimized at our level of calculation.

As shown in Table 6, the DPE's of the C-H_i bonds are systematically larger than the DPE's of the C-H_g bond. The difference is however very small for the two C-H bonds of dimethyl ether (0.7 kJ mol^{-1}) but is thought to be significant. For the fluorinated ethers, this difference

ranges between 4 and 10 kJ mol⁻¹. The only exception is predicted for the CHF₂OCHF₂ molecule where the DPE value of the C–H_f bond is by 6 kJ mol⁻¹ smaller than the DPE of the C–H_g bond. This may be accounted for by the fact that the most stable deprotonated species is characterized by the D and not the A conformation (Fig. 2).

Our results indicate that substitution of H by F atoms exerts a great influence on the proton donor ability of the CH groups. Indeed, substitution of five H atoms by five F atoms lowers the corresponding DPE by ca. 214 kJ mol⁻¹. Theoretical calculations have shown that the acidity of CH₃–CH₃ is increased by 192 kJ mol⁻¹ by pentafluoro-substitution [47]. Comparison with other fluorinated ethane derivatives, more specifically the substitution effect on both C atoms, is difficult because several substituted anions are unstable and decompose into a fluoro anion and the relevant substituted ethylene [47].

In the present work, we have calculated the DPE of the CH groups bonded to the C1 and C2 atoms and it is interesting to compare the substitution effects on the C1X₃ and OC2X₃ groups. Results of Table 6 show that the DPE's of the C1H₃ groups of the *gauche* conformers decreases by 45, 76 and 87 kJ mol⁻¹ with respect to the unsubstituted molecule if OCH₂F, OCHF₂ and OCF₃ substituents, respectively, are implanted on the ether.

We can also consider the direct effect of F substitution on the DPE of the C1H₃ group. When this group is substituted by one or two F atom(s), the DPE tends to decrease by 46 and 106 kJ mol⁻¹, respectively. Thus monofluoro-substitution has exerted a similar influence on the DPE of the C1H and C2H bonds but that difluoro-substitution induces a larger influence on the DPE of the C1H group. Still larger differences are observed for C1H₃OC2F₃ compounds where the DPE of the C1H bond is found to be reduced by 128 kJ mol⁻¹ in the C1H₂FOC2F₃ molecule and by 213 kJ mol⁻¹ in the C1HF₂OCF₃ one.

In addition, results listed in Table 6 reveal that for a given pair of two conformers, the highest acidity of the CH bond parallels a larger σ*(C–H) occupation.

An increase in the s-character of the C-center at the departing H is expected to increase the acidity of the corresponding C–H bond. In the hydrocarbon series, there is increase of acidity of 62 kJ mol⁻¹ on going from C₂H₆ to C₂H₄ and of 123 kJ mol⁻¹ from C₂H₄ to C₂H₂ [48]. As indicated in Fig. 5, there is a very rough correlation between the DPE of all the compounds investigated in this work and the % s-character of the C at the H involved in the protonation process:

$$\text{DPE} = 2470 - 30.47(\%s \text{ C–H}) \quad (r = 0.8745) \quad (2)$$

4. Concluding remarks and perspectives

The present study deals with a theoretical study carried out at the B3LYP/6-311++G(d,p) level of the conformation, proton affinities of the O atoms and the deprotonation enthalpies of the CH bonds of fluorinated dimethyl ethers.

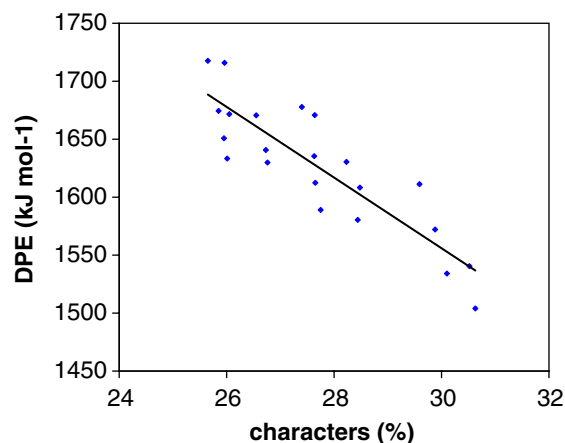


Fig. 5. DPE (kJ mol⁻¹) as a function of the %s-character of the C–H bond.

The main factor governing the conformation of the molecules is the hyperconjugative effect taking place from the lone pair of the O atom to the σ* orbital of the C–F bond in *gauche* position. In a further study, we will investigate the interaction between DMFE and water or other guest molecules. Dimethyl ether interacts with water to give OH...O bonds of medium strength (23 kJ mol⁻¹) [37] and from the strong decrease in basicity resulting from fluoro-substitution, much weaker OH...O hydrogen bonds between water and the substituted ethers can be predicted. Further, dimethyl ethers substituted by four or five F atoms are characterized by DPE ranging between 1590 and 1504 kJ mol⁻¹. Such acidities are similar to the ones of classical proton donors in hydrogen bonds studies such as C₂H₅OH (1580 kJ mol⁻¹), C₂H₂F₂OH (1533 kJ mol⁻¹), CH₂F₃OH (1514 kJ mol⁻¹) [17]. Despite the fact that DPE (or pK_a in solution) is not the sole factor in determining hydrogen bond geometries or energies, the existence of hydrogen bonds involving the CH group of fluoro substituted ethers can be anticipated from the present study. It is worth mentioning that the proton donor ability of the C–H bond of dimethyl ether has been discussed in two recent papers [49,50] Dimethyl ether is able to form a homodimer where the two molecules are held together through C–H...O hydrogen bonds [49]. Further, it has been shown that the more strongly bounded structure of the complex between dimethyl ether and hydrogen peroxide contains a OH...O bond, along with a blue-shifting C–H...O bond that contributes to the stabilization of the structure [50].

Acknowledgements

We are indebted to the KULeuven Research Council (GOA and DB programs) and the Flemish Fund for Scientific Research (FWO-Vlaanderen) for continuing support.

References

- [1] G. Trudeau, J.M. Dumas, P. Dupuis, M. Guérin, C. Sandorfy, Top. Curr. Chem. 93 (1980) 91.

- [2] N.P. Franks, W.R. Lieb, *Nature* 367 (1994) 607, and references therein.
- [3] C. Sandorfy, *Anesthesiology* 101 (2004) 1225.
- [4] C. Sandorfy, *J. Mol. Struct.* 708 (2004) 3.
- [5] C. Sandorfy, *Collect. Czech. Chem. Commun.* 70 (2005) 539.
- [6] For reviews of hydrogen bonding in weakly bound systems, see: G.R. Desiraju, T. Steiner, *The Weak Hydrogen Bond in Structural Chemistry and Biology*, Oxford University Press, New York, 1999.
- [7] E.S. Kryachko, Th. Zeegers-Huyskens, *J. Phys. Chem. A* 105 (2001) 7118.
- [8] K.S. Rutkowski, P. Rodziewicz, S.M. Melikova, W.A. Herrebout, B.J. van der Veken, A. Koll, *Chem. Phys.* 313 (2005) 225.
- [9] B. Czarnik-Matusiewicz, D. Michalska, C. Sandorfy, Th. Zeegers-Huyskens, *Chem. Phys.* 322 (2006) 331.
- [10] P.E. Balonga, V.J. Kowalewski, R.H. Contreras, *Spectrochim. Acta* 44A (1988) 818.
- [11] A. Pfeiffer, H.G. Mack, H.J. Oberhammer, *J. Am. Chem. Soc.* 120 (1998) 6384.
- [12] C. Zhao, P.L. Polavarapu, H. Grosenik, V. Schurig, *J. Mol. Struct.* 550 (2000) 105.
- [13] A. Sekiya, S. Misaki, *Chemtech* 26 (1996) 44.
- [14] L. Chen, S. Kutsuna, K. Tokuhashi, A. Sekiya, *J. Phys. Chem. A* 110 (2006) 12845.
- [15] A.K. Chandra, T. Uchimaru, *Chem. Phys. Lett.* 334 (2001) 200.
- [16] N. Hartz, G. Rasui, G.A. Olah, *J. Am. Chem. Soc.* 115 (1993) 1277.
- [17] S.L. Lias, J.E. Bartmess, J.F. Liebman, J.L. Holmes, R.D. Levin, W.G. Mallard, Gas-phase ion and neutral thermochemistry, *J. Phys. Chem. Ref. Data* 117 (Suppl. 1) (1988) 1988.
- [18] A.K. Chandra, M.T. Nguyen, T. Uchimaru, Th. Zeegers-Huyskens, *J. Phys. Chem. A* 103 (1999) 8853.
- [19] G.A. DiLabio, D.A. Pratt, A.D. LoFaro, J.S. Wright, *J. Phys. Chem. A* 103 (1999) 1653.
- [20] A.K. Chandra, D. Michalska, R. Wysokinski, Th. Zeegers-Huyskens, *J. Phys. Chem. A* 108 (2004) 9593.
- [21] M.D. Liptak, G.C. Shields, *Int. J. Quant. Chem.* 105 (2005) 580, and references therein.
- [22] A.E. Reed, L.A. Curtiss, F. Weinhold, *Chem. Rev.* 88 (1988) 899.
- [23] M.J. Frisch, G.W. Trucks, H.B. Schlegel, G.E. Scuseria, M.A. Robb, J.R. Cheeseman, J.A. Montgomery, T. Vreven, K.N. Kudin, J.C. Burant, S.S. Iyengar, J. Tomasi, V. Barone, C.B. Mennucci, M. Cossi, G. Scalmani, N. Rega, G.A. Petersson, H. Nakatsuji, M. Hada, M. Ehara, K. Toyota, J. Hasegawa, M. Ishida, T. Nakajima, Y. Honda, O. Kitao, H. Nakai, M. Klene, X. Li, J.E. Knox, H.P. Hratchian, J.B. Cross, V. Bakken, C. Adamo, J. Jaramillo, R. Gomperts, R.E. Stratman, O. Yazyev, A.J. Austin, R. Cammi, C. Pomelli, J.W. Ochterski, P.Y. Ayala, K. Morokuma, G.A. Voth, P. Salvador, J.J. Dannenberg, V.G. Zakrzewski, S. Dapprich, A.D. Daniels, M.C. Strain, O. Farkas, D.K. Malick, A.D. Rabuck, K. Raghavachari, J.B. Foresman, J.V. Ortiz, Q. Cui, A.G. Baboul, S. Clifford, J. Cioslowski, B.B. Stefanov, G. Liu, A. Liashenko, P. Piskorz, I. Komaromi, R.L. Martin, D.J. Fox, T. Keith, M.A. Al-Laham, C.Y. Peng, A. Nanayakkara, M. Challacombe, P.M.W. Gill, B. Johnson, W. Chen, M.W. Wong, C. Gonzales, J.A. Pople, Gaussian 03, revision B. 03; Gaussian Inc., Pittsburgh, PA, 2004.
- [24] P. Deslongchamps, *Stereochemical Effects in Organic Chemistry*, Pergamon, Oxford, 1983.
- [25] See for example: P.v.R. Schleyer, A. Kos, *Tetrahedron* 39 (1983) 1141.
- [26] A.E. Reed, C. Schade, P.v.R. Schleyer, P.V. Kamath, J.J. Chandrasekar, *J. Chem. Soc. Chem. Commun.* 67 (1988).
- [27] U. Salzner, P.v.R. Schleyer, *J. Am. Chem. Soc.* 115 (1993) 10231, and references therein.
- [28] I.V. Alabugin, T.A. Zeidan, *J. Am. Chem. Soc.* 124 (2002) 3175, and references therein.
- [29] L. Goodman, V. Pophistic, *Chem. Phys. Lett.* 259 (1996) 287.
- [30] V. Pophistic, L. Goodman, N.J. Guchhait, *J. Phys. Chem. A* 101 (1997) 4290.
- [31] C. Castiglioni, M. Gussoni, G. Zerbi, *J. Mol. Struct.* 198 (1989) 145.
- [32] M. Gussoni, C. Catiglioni, M.N. Ramos, M. Rui, G. Zerbi, *J. Mol. Struct.* 224 (1990) 445.
- [33] M. Gussoni, C. Castiglioni, *J. Mol. Struct.* 521 (2000) 1.
- [34] S. Radice, P. Toniolo, M. Avataneo, U. De Patto, G. Marchionni, C. Castiglioni, M. Tommasini, G. Zerbi, *J. Mol. Struct.* 710 (2004) 151.
- [35] A.J. Barnes, T.R. Beech, *Chem. Phys. Lett.* 94 (1983) 568.
- [36] B.J. van der Veken, W.A. Herrebout, R. Szostak, D.M. Shchepkin, Z. Havlas, P. Hobza, *J. Am. Chem. Soc.* 123 (2001) 12290.
- [37] S. Vijayakumar, P. Kollandaivel, *J. Mol. Struct.* 734 (2004) 157.
- [38] F. Bohlmann, *Angew. Chem.* 69 (1957) 641.
- [39] G.A. Jeffrey, J.H. Yates, *J. Am. Chem. Soc.* 101 (1979) 820.
- [40] J.R. Durig, G.A. Lin, B.J. van der Veken, *J. Struct. Chem.* 4 (1993) 103.
- [41] J. Nagakawa, H. Kato, M. Hayashi, *J. Mol. Spectrosc.* 90 (1981) 467.
- [42] R. Kühn, D. Christen, H.G. Mack, D. Konikowski, R. Minkwitz, H. Oberhammer, *J. Mol. Struct.* 376 (1996) 217.
- [43] D.C. Mc Kean, A. Kindness, N. Wilkie, W.F. Murphy, *Spectrochim. Acta* 52 A (1996) 445, and references therein. The sum of the experimental infrared intensities for the six fundamental CH₃ stretching vibrations in dimethyl ether comprises between 253 and 294 km mol⁻¹ (average value = 268 km mol⁻¹). The value calculated at the MP2/6-31G(d) level is 272 km mol⁻¹, very near to the experimental value. Our B3LYP/6-311++G(d,p) calculations give a value of 324 km mol⁻¹, which is ca 20% too large and only indicate qualitative trends. In contrast, frequencies are much better predicted by B3LYP calculations. The experimental frequencies of the CH₃ stretching vibrations in dimethyl ether comprise between 2986 and 2925 cm⁻¹ (Ref. [35]). The MP2 calculations predict these frequencies between 3218 and 3051 cm⁻¹, giving an average scale factor of 0.938. The scale factor extracted from our B3LYP calculations is 0.975, in much better agreement with the experiments..
- [44] P. Redfern, S. Scheiner, *J. Comput. Chem.* 6 (1985) 68.
- [45] J.-L. Abboud, J. Elguero, D. Liotard, M. Essefar, M. El Mouhtadi, R.W. Taft, *J. Chem. Soc. Perkin Trans. 2* (1990) 565.
- [46] K.B. Wiberg, M. Marquez, H. Castejon, *J. Org. Chem.* 59 (1994) 6817.
- [47] S.D. Wetmore, R. Schofield, D.M. Smith, L. Radom, *J. Phys. Chem. A* 105 (2001) 8718.
- [48] J.F. Gal, P.C. Maria, in: R.W. Taft (Ed.), *Progress in Physical Organic Chemistry*, vol. 17, John Wiley & Sons Inc., 1990, p. 159.
- [49] C. Bleiholder, D.B. Werz, H. Köppel, R. Gleiter, *J. Am. Chem. Soc.* 128 (2006) 2666.
- [50] M. Solimannejad, S. Scheiner, *Chem. Phys. Lett.* 429 (2006) 38.